Imaging a toroidal vortex and the Rayleigh–Taylor instability, and the transition between them: A Get Wet 2019 Report

Abhishek L. Kumar [a,*]

ATLS 5151 – 001: Flow Visualization, Fall 2019

[a]*University of Colorado Boulder, 1111 Engineering Drive, Boulder, CO 80309*

1. Introduction

The goal was to try and capture an image demonstrating two flow phenomena at the same time. My secondary, personal goal was to learn more about photography and the techniques that go with photography, and of course, post processing, to add an artistic touch, for both of which, I was a novice at the time Figure 1 was captured. This assignment (Get Wet 2019) is my first imaging assignment. The purpose of this report is to adequately document the steps involved in taking my Get Wet 2019 image and to include the imaging techniques and processing techniques used, and the science behind the image. This report attempts to explain (on a surface level) the definition of a vortex, a toroidal vortex (vortex ring), and the Rayleigh–Taylor instability, and the reasons for their formation.

2. Flow Phenomena

For the flow physics, lets start with vortices. A *vortex* is a fluid (gas or liquid) moving in circles along an axis, called the *vortex line*. When the vortex line is a curve, specifically a circle or an ellipse, a *toroidal vortex* is created. It is basically fluid revolving around an axis that is circular. As depicted in the Figure 1 and in FIG 4 in the article by Kreuger & Gharib (2003), imagine a hurricane/typhoon (vortex northern hemisphere) and a cyclone (vortex in the southern hemisphere) next to each other. Since the fluid is revolving around in different rotational directions, the fluid closest to the two storms is going in the same direction, hence they move forward in that direction. At any given point, a cross section (cut in half (plane along the direction of motion) of the toroidal vortex reveals the same analogy used as the storms. The *Rayleigh–Taylor instability* happens when a fluid of higher density (preferably lower quantity, like a droplet) sinks due to gravity in a fluid of lower density. The bulk of the higher density fluid falls faster than the edges, and based on the state of the lower density fluid (stagnant or moving), different patterns are created. For a stabilized bulk fluid, the instability would be in the form of something similar to a mushroom cloud, due to the shear on the outer layers (due to friction).

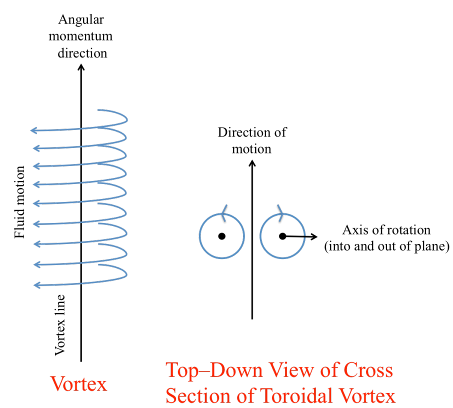

Figure 1: Motion characteristics of a Toroidal Vortex

* Corresponding author

3. Flow Visualization Technique

Smoke was used as a tracer for this assignment. The vaporizer pen was manufactured by Vaporesso ("Tarot Baby"). The fluid used to produce the vapor was made by the American Vapor Group. The composition of the fluid was 90% Vegetable Glycerin, 10% Propylene Glycol, and water. An LED panel, provided by Dr. Hertzberg, was used as the lighting source. The panel was located orthogonal (90º) to the image plane, and placed on the right hand side. Figure 2 described the setup used. A tripod was not used. The image was captured in a closed environment, with still air (achieved by turning of the HVAC system, and having a closed system), to allow the motion of only the vapor. Otherwise, the stability of the vortex ring and its subsequent diffusion/ decay would not be natural, and will be influenced by factors such as air draft and easily collapses the structure/ hastens the diffusion process, which would make it harder to image the flow phenomena in this case. This technique made sure to isolate the motion of the ring to around 1 inch per second. The direction of the motion of the ring was orthogonal (90º) to the direction of lighting.

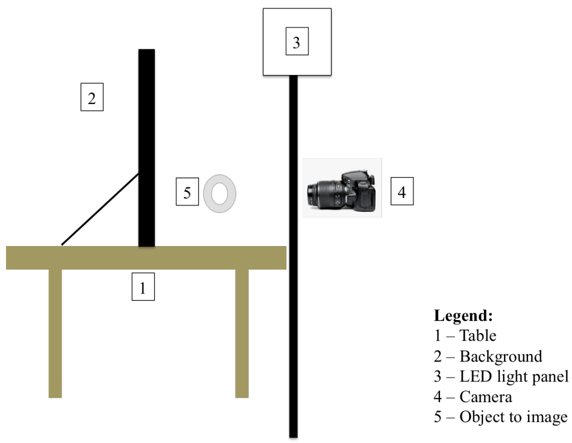

Figure 2: Setup used for imaging

4. Photography Technique

The Camera used was a Nikon D3200 with an 18–55 lens (DSLR digital camera). As shown in Figure 2, the camera was hand–held, and kept orthogonal to the lighting source. The required parameters are listed and calculated as follows:

1. *Lens Specs* – Focal length: 22 mm, F number (f/): 5
2. *Exposure specifications* – Shutter Speed: 1/30 sec, ISO: 720, Aperture size = 4.4mm[(1)]
3. *Camera and Image* – Nikon 3200 DSLR (digital), Original (w x h) = 6016 x 4000 pixels, Final (w x h) = 4553 × 3297 pixels
4. *Distance of object (to lens)*: 7.88 in[(2)]
5. *Field of View*: 5.52 in x 8.3 in[(3)].
6. *Final cut processing (Photoshop)*: The self-explanatory Figure 3 summarizes the adjustments made in Photoshop of the original image, and Figure 4 shows the image before and after processing. The processing settings were different for the first post made. After reviewing the feedback from class and Dr. Hertzberg in the critique sessions, the original image was processed again, to incorporate changes. The only settings listed/ shown in this document are for the final posted version of the image.

Reasons for choosing the mentioned settings: As mentioned in Section 3, due to the mobile nature of the vortex ring, a faster shutter speed, and larger aperture was chosen, to minimize motion blur. The ISO was in a decent middle range, and was automatically set by the camera for those specifications. After the vortex ring formed, the image was taken after 4 seconds elapsed, to allow the vortex ring to slow down and break down into instability. The particular ring shown in Figure 4 was mobile as a toroidal vortex for about 3 seconds, and then broke into the Rayleigh–Taylor instability. Another second was given after this, to allow the instability to morph into its different stages. This stage specifically resembles the stage depicted by Wang & Roger (2001) at t' = 0.004 with l = 1000 and 45º in FIG 6 of the article.

Calculations:

[1]Aperture size: $D = F/f\# = 22 \text{ mm} / 5 = \underline{4.4 \text{ mm}}$

[2]Distance to lens: a non-conventional formula was used:

$$Ob = \frac{F(\text{mm}) \times \text{Real Height (mm)} \times \text{Image Height (Pixels)}}{\text{Object Height (Pixels)} \times \text{Sensor Height (mm)}} = \frac{20 \times 88.9 \times 6016}{3466.8 \times 15.4} = 200.35 \text{ mm} = \underline{7.88 \text{ in}}$$

Angle of view (degrees):

$$= \left(\arctan\left[\text{Sensor Width (mm)}/2 \times F(\text{mm})\right]\right) = 27.8^{\circ}$$

$$= \left(\arctan\left[\text{Sensor Height (mm)}/2 \times F(\text{mm})\right]\right) = 19.29^{\circ}$$

[3]Hence Field of View =

$$2 \times (\tan(\text{Angle of View}) \times Ob) = 2 \times (\tan(19.29) \times 200.35) = 140.24 \text{ mm } = \underline{5.52 \text{ in}}$$

$$2 \times (\tan(\text{Angle of View}) \times Ob) = 2 \times (\tan(27.8) \times 200.35) = 211.26 \text{ mm } = \underline{8.3 \text{ in}}$$

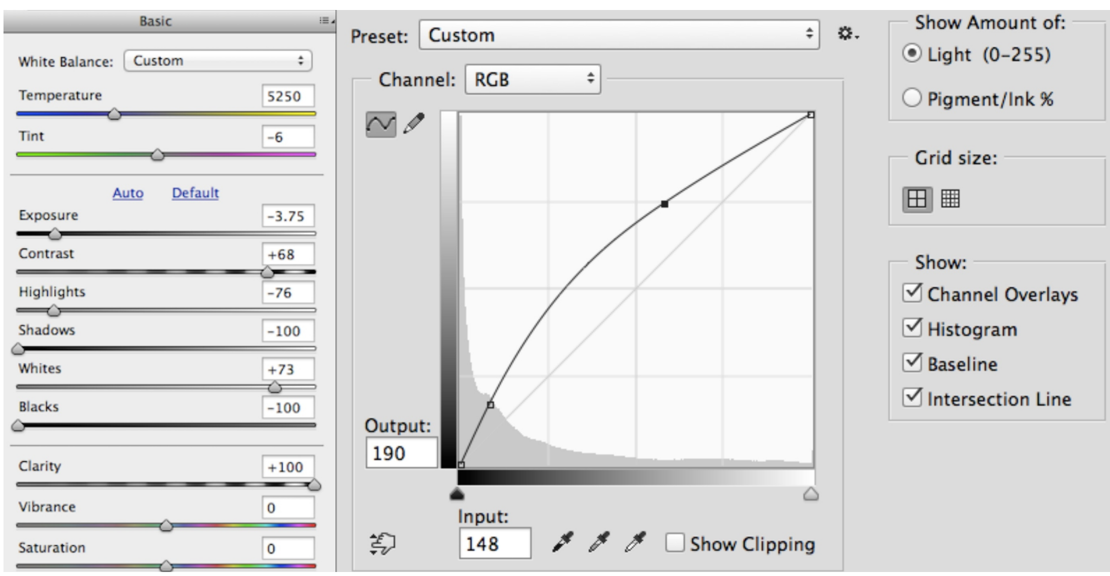

Figure 3: (a) Menu on the left was used first and then (b) curves on the right was edited as shown

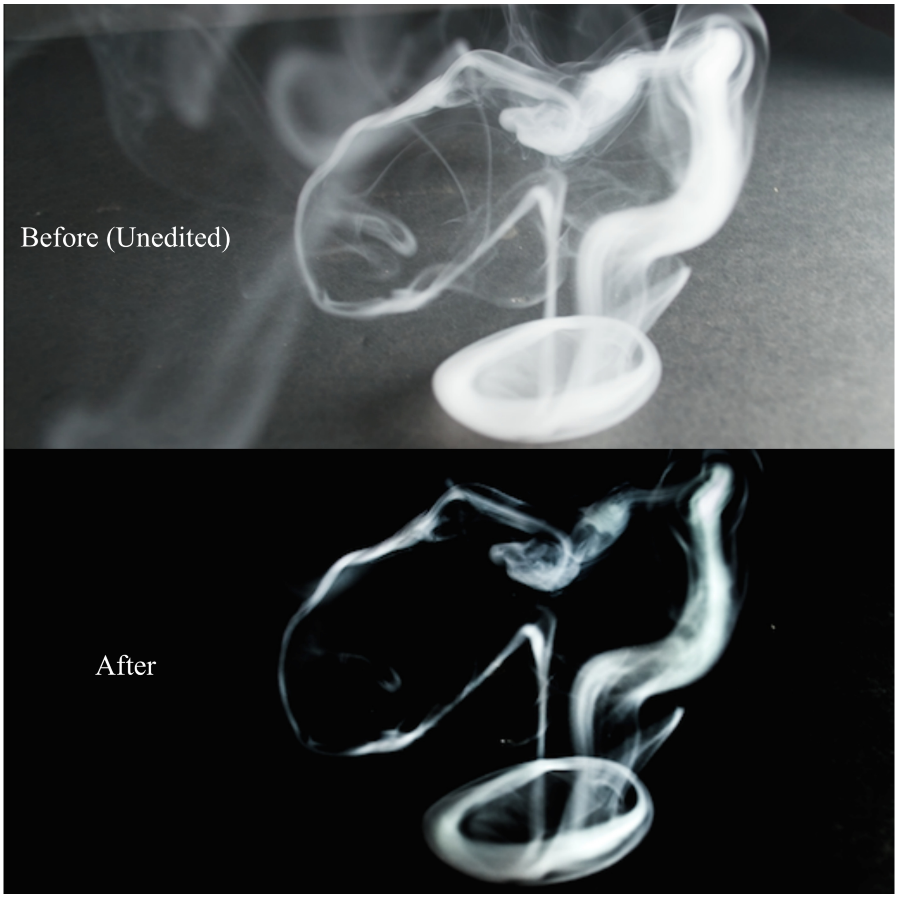

Figure 4: Unedited (top) and Edited (bottom) versions of Image

5. Image Characteristics

As seen in Figure 4, we can see the residual vortices (upper right and center of object), and the mushroom cloud (bottom) demonstrates the vapor in one of its final stages of the Rayleigh–Taylor instability. The sinking vapor had enough velocity to form another vortex ring stemming from the mushroom cloud, but the cloud collapsed onto the table and dissipated before that could take place. I like that we can see the transition as well as both the flow phenomena mentioned above. However, it could have been in focus a little more, especially near the mushroom cloud and the remnant vortex, and would like to improve quality of future images with better photographing and post–processing techniques. The intent to capture both the processes was fulfilled with this image. Going forward, I would like to further understand the transitional phase and why the lines leading into the instability are laminar. I would also like to study the wobbling effect produced by using a non circular hole.

6. References:

Wang C., Roger A. (2001), "Instabilities and Clumping in Type Ia Supernova Remnants", *The Astrophysical Journal*, 549: p1119 – 1134.

Kreuger S. P., Gharib M. (2003), "Significance of Vortex ring Formation to the Impulse and Thrust of a Starting Jet", *Physics of Fluids*, 15: 1271.